

# Neural Stochastic Partial Differential Equations

Cristopher Salvi      Maud Lemerrier

October 22, 2021

## Abstract

*Stochastic partial differential equations* (SPDEs) are the mathematical tool of choice to model complex spatio-temporal dynamics of systems subject to the influence of randomness. We introduce the *Neural SPDE* model providing an extension to two important classes of physics-inspired neural architectures. On the one hand, it extends all the popular neural – ordinary, controlled, stochastic, rough – differential equation models in that it is capable of processing incoming information even when the latter evolves in an infinite dimensional state space. On the other hand, it extends Neural Operators – recent generalizations of neural networks modelling mappings between functional spaces – in that it can be used to learn complex SPDE solution operators  $(u_0, \xi) \mapsto u$  depending simultaneously on an initial condition  $u_0$  and on a stochastic forcing term  $\xi$ , while remaining resolution-invariant and equation-agnostic. A Neural SPDE is constrained to respect real physical dynamics and consequently requires only a modest amount of data to train, depends on a significantly smaller amount of parameters and has better generalization properties compared to Neural Operators. Through various experiments on semilinear SPDEs with additive and multiplicative noise (including the stochastic Navier-Stokes equations) we demonstrate how Neural SPDEs can flexibly be used in a supervised learning setting as well as conditional generative models to sample solutions of SPDEs conditioned on prior knowledge, systematically achieving in both cases better performance than all alternative models.

## 1 Introduction

Interest in combining differential equations and deep learning has recently given rise to a large variety of neural differential equation architectures such as neural ordinary (Chen et al., 2018), stochastic (Li et al., 2020a), controlled (Kidger et al., 2020) and rough (Morrill et al., 2021) differential equations (Neural ODEs, SDEs, CDEs, RDEs). These models can be seen as continuous analogues of some classical neural network architectures (ResNets, RNNs etc.) and are emerging as leading machine learning tools for modelling various kinds of temporal dynamics with finite dimensional state space.

Many dynamical systems though, evolve in an infinite dimensional state space of functions and can best be described using the language of partial differential equations (PDEs). Neural Operators (Kovachki et al., 2021; Li et al., 2020c,b,d) are generalizations of neural networks offering an elegant way to learn mappings between spaces of

functions, which makes them an attractive option for modelling PDE-dynamics. However, deterministic PDEs fail to incorporate randomness into the system they describe. In many cases the presence of noise leads to new phenomena, both at the mathematical and the physical level, generally describing more complex and realistic dynamics than the ones arising from deterministic PDEs.

*Stochastic partial differential equations* (SPDEs) are the mathematical tool of choice to model many physical, biological and economic systems subject to the influence of randomness, be it intrinsic (e.g. quantifying uncertainty) or extrinsic (e.g. modelling environmental random perturbations). Examples include the *Kardar–Parisi–Zhang (KPZ) equations* for random interface growth modelling for instance the propagation of a forest fire from a burnt region to an unburnt region (Hairer, 2013), the  $\Phi^4$ -models describing phase transitions of ferromagnets and superconductors near critical temperatures (Kleinert & Schulte-Frohlinde, 2001), or the *stochastic Navier-Stokes equations* modelling the dynamics of a turbulent fluid flow under the presence of local random fluctuations (Mikulevicius & Rozovskii, 2004). For an introduction to SPDEs see (Hairer, 2009); a comprehensive textbook is (Holden et al., 1996).

Whilst Neural Operators can certainly be used to learn operators mapping the initial condition  $u_0$  or a known forcing term  $\xi$  to the solution  $u$  of a PDE, they are not designed to handle SPDEs where solutions depend simultaneously on an initial condition  $u_0$  representing prior knowledge of the system and on a stochastic forcing  $\xi$ . Using the notion of mild solution to an SPDE and some basic semigroup theory, we resolve this issue and introduce the *neural stochastic partial differential equation* (Neural SPDE) model. A Neural SPDE is a flexible model that can be used

1. in a supervised learning setting to model the operator  $(u_0, \xi) \mapsto u$  (assuming the forcing term  $\xi$  is observed);
2. as a generator in a conditional generative modelling setting to produce randomly sampled solutions matching the distributional behaviour of some observed solutions of an underlying unknown SPDE, conditioned on  $u_0$ .

We perform experiments on various semilinear SPDEs with additive and multiplicative stochastic forcing, including the stochastic Navier-Stokes equations. The outcomes illustrate three key aspects of our model. One it is resolution-invariant, which means that even if trained on a lower resolution it can be directly evaluated on a higher resolution (zero-shot super-resolution). Two, it does not require knowledge of the exact form of the underlying SPDE. Three, it is constrained to respect real physical dynamics and consequently requires only a modest amount of training data, depends on a significantly smaller amount of parameters and has better generalization properties compared to all alternative (neural differential equations and operators based) models.

## 2 Related work

In this section we provide a brief introduction to the most popular neural differential equation models for temporal dynamics in finite dimensions as well as to Neural

Operators, a recent generalization of neural network to infinite dimensional spaces of functions. Let  $T > 0$  and  $d, d_u, d_\xi, d_h \in \mathbb{N}$ .

## 2.1 Neural ordinary differential equations

A neural ordinary differential equation (Neural ODE), as popularised by (Chen et al., 2018), is a parametric model with initial input  $u_0 \in \mathbb{R}^{d_u}$  consisting of

- a lift from the input state space  $\mathbb{R}^{d_u}$  to a hidden state  $\mathbb{R}^{d_h}$  (with  $d_h$  chosen by the user) parameterized via a first neural network  $\ell_\theta : \mathbb{R}^{d_u} \rightarrow \mathbb{R}^{d_h}$ ,
- a vector field of an ODE evolving in the hidden state modelled via a second neural network  $f_\theta : \mathbb{R}^{d_h} \rightarrow \mathbb{R}^{d_h}$  (with some minimum Lipschitz regularity),
- and a projection from the hidden state back to the original space via a final (usually linear) readout map  $\pi_\theta : \mathbb{R}^{d_h} \rightarrow \mathbb{R}^{d_u}$ .

The forward pass of a Neural ODE is as follows

$$z_0 = \ell_\theta(u_0), \quad z_t = z_0 + \int_0^t f_\theta(z_s) ds, \quad u_t = \pi_\theta(z_t). \quad (1)$$

The integral in (1) can be evaluated numerically via a call to an ODE solver of choice

$$z_t \approx \text{ODESolve}(z_0, f_\theta, t)$$

The output  $u_t$  is then fed to a loss function (mean squared, cross entropy etc.) and trained via stochastic gradient descent in the usual way. As described in Chen et al. (2018), backpropagation can be done efficiently via adjoint methods Pontryagin (1987) by solving additional ODEs for the gradients of the loss instead of backpropagating through the operations of the ODE solver. Once the parameters  $\theta$  have been learnt, the solution of eq. (1) it's determined by the initial condition  $u_0$ , and there is no direct mechanism for adjusting the trajectory based on data that arrives at later times (Ciccone et al., 2018).

## 2.2 Neural controlled differential equations

Controlled differential equations (CDEs) (Lyons, 1998, 2014; Lyons et al., 2007) allow to resolve this issue by incorporating incoming information into the dynamics of an ODE. Given an initial condition  $u_0 \in \mathbb{R}^d$  and some time-dependent information (usually a time series) interpolated into a continuous path  $\xi : [0, T] \rightarrow \mathbb{R}^{d_\xi}$  of bounded variation, a Neural CDE (Kidger et al., 2020) consists of the same neural networks  $\ell_\theta, f_\theta, \pi_\theta$  as in a Neural ODE, as well as an additional matrix-valued neural network  $g_\theta : \mathbb{R}^{d_h} \rightarrow \mathbb{R}^{d_h \times d_\xi}$

(with minimal Lipschitz regularity)<sup>1</sup>. The forward pass of a Neural CDE is as follows

$$z_0 = \ell_\theta(u_0), \quad z_t = z_0 + \int_0^t f_\theta(z_s)ds + \int_0^t g_\theta(z_s)d\xi_s, \quad u_t = \pi_\theta(z_t). \quad (2)$$

where the integral is interpreted in the Riemann–Stieltjes sense. In Kidger et al. (2020), the control  $\xi$  is obtained using cubic spline interpolation on the original data so that the term " $d\xi_s$ " can be interpreted as " $\dot{\xi}_s ds$ ". Therefore eq. (2) simply becomes an ODE and forward and backward passes can be carried out as in a Neural ODE model. In (Morrill et al., 2021) the authors discuss how to relax the differentiability assumption on  $\xi$  and propose the neural rough differential equation (Neural RDE) model as an extension to Neural CDEs.

### 2.3 Neural stochastic differential equations

Neural stochastic differential equations (Neural SDEs) are special classes of Neural CDEs where the control  $\xi$  is a sample path from a  $\mathbb{R}^{d_\xi}$ -dimensional Brownian motion and where the integral is a stochastic integral understood in the Stratonovich sense  $\int_0^t g_\theta(z_s) \circ d\xi_s$ . Neural SDEs can be used as generative models (trained either as VAEs or GANs) for path-valued random variables (Kidger et al., 2021b,a).

Neural ODEs, CDEs, SDEs, RDEs are elegant continuous models for describing dynamics of systems where inputs  $u_0, \xi$  and outputs  $u$  take their values in finite dimensional spaces  $\mathbb{R}^{d_u}, \mathbb{R}^{d_\xi}$ . However, they can't be used in situations where the state spaces of the control and of system are infinite dimensional, as it is the case when one studies the dynamics described by partial differential equations (PDEs).

### 2.4 Neural Operators

Neural Operators (Kovachki et al., 2021; Li et al., 2020c,b) are generalizations of neural networks offering an elegant way to model mappings between spaces of functions. Contrary to the previous differential equation models, in Neural Operators the initial condition is treated as a function  $u_0 : \mathcal{D} \rightarrow \mathbb{R}^d$  from a spatial domain  $\mathcal{D}$  to  $\mathbb{R}^d$ . A Neural Operator can then be used to learn the mapping  $u_0 \mapsto u$  or the mapping  $\xi \mapsto u$ , where  $u : [0, T] \times \mathcal{D} \rightarrow \mathbb{R}^{d_u}$  is the solution of an underlying unknown PDE with initial condition  $u_0 : \mathcal{D} \rightarrow \mathbb{R}^{d_u}$  and spatio-temporal forcing term  $\xi : [0, T] \times \mathcal{D} \rightarrow \mathbb{R}^{d_\xi}$ . To work with them numerically, the user has access to  $u_0$  via its pointwise evaluations on a discretization  $D$  of the spatial domain  $\mathcal{D}$  and to the forcing term  $\xi$  through its pointwise evaluations on a discretized spatio-temporal grid  $\mathcal{T} \times D$ , where  $\mathcal{T} = \{0 = t_0 < t_1 < \dots < t_n = T\}$ .

Contrary to prior work attempting to merge PDEs and deep learning, Neural Operators do not require knowledge of the exact form of the underlying PDE, they are resolution-invariant<sup>2</sup> so even if trained on a coarser grid they can be evaluated on a finer grid

<sup>1</sup>In (Kidger et al., 2020) the control path  $\xi$  is "augmented-with-time" to form a new path  $\hat{\xi}_t = (t, \xi_t) \in \mathbb{R}^{d_\xi+1}$  so that the update in eq. (2) can be rewritten more compactly as  $z_t = z_0 + \int_0^t h_\theta(z_s)d\hat{\xi}_s$ , where  $h_\theta : \mathbb{R}^{d_h} \rightarrow \mathbb{R}^{d_h \times (d_\xi+1)}$  is another neural network.

<sup>2</sup>Neural CDEs, SDEs, RDEs are time-resolution invariant but clearly not space-resolution invariant.

without giving up on accuracy, and they achieve superior performance compared to previous deep-learning-based PDE solvers.

Given an input function  $u^{\text{in}} : [0, T] \times \mathcal{D} \rightarrow \mathbb{R}^{d_u}$ , a Neural Operator with  $M$  layers is defined as an iterative architecture such that for any  $t \in [0, T]$ ,  $x \in \mathcal{D}$ ,  $k = 1, \dots, M$

$$z^0(t, x) = L_\theta(u^{\text{in}}(t, x)), \quad z^k = N_\theta^k(z^{k-1}), \quad u^{\text{out}}(t, x) = \Pi_\theta(z^M(t, x)), \quad (3)$$

where  $L_\theta : \mathbb{R}^{1+d_u} \rightarrow \mathbb{R}^{d_h}$  and  $\Pi_\theta : \mathbb{R}^{d_h} \rightarrow \mathbb{R}^{d_u}$  are feedforward neural networks and each  $N_\theta^k$  is a parametric operators defined for any function  $z : [0, T] \times \mathcal{D} \rightarrow \mathbb{R}^{d_h}$  as

$$N_\theta^k(z)(t, x) := \sigma \left( A_\theta^k z(t, x) + b_\theta^k + \int_0^t \int_{\mathcal{D}} \mathcal{K}_\theta^k(t, s, x, y) z(s, y) ds dy \right) \quad (4)$$

where  $A_\theta^k \in \mathbb{R}^{d_h \times d_h}$ ,  $b_\theta^k \in \mathbb{R}^{d_h}$ ,  $\mathcal{K}_\theta^k : [0, T]^2 \times \mathcal{D}^2 \rightarrow \mathbb{R}^{d_h \times d_h}$  is a matrix-valued kernel and  $\sigma$  is a non-linear activation function.

**Remark 1** *An alternative architecture (one-step-ahead Neural Operator) attempts to model the mapping  $u^{\text{in}}(t_{i-1}, \cdot) \rightarrow u^{\text{out}}(t_i, \cdot)$  for  $i = 1, \dots, n$ , rather than modelling  $u^{\text{in}} \rightarrow u^{\text{out}}$  on the whole time interval  $[0, T]$ . The architecture is very similar to the above, with the exception that all functions are only evaluated at a spatial input  $x \in \mathcal{D}$ , the kernel  $\mathcal{K}_\theta^k : \mathcal{D}^2 \rightarrow \mathbb{R}^{d_h \times d_h}$  acts only on space, and the integral is only in space.*

## 2.5 Fourier Neural Operators

Among all kinds of Neural Operators Kovachki et al. (2021); Li et al. (2020c,b), Fourier Neural Operators (FNO) stand out because of their easier parametrization whilst maintaining similar computational efficiency and accuracy performance for learning complex PDE operators (Li et al., 2020d). In a FNO, the kernel  $\mathcal{K}_\theta^k$  is assumed to be stationary so that  $\mathcal{K}_\theta^k(t, s, x, y) = \mathcal{K}_\theta^k(t - s, x - y)$ . With this assumption, the double integral in eq. (4) becomes a space-time convolution, denoted by  $*_{d+1}$ , so that

$$N_\theta^k(z)(t, x) = \sigma \left( A_\theta^k z(t, x) + b_\theta^k + (\mathcal{K}_\theta^k *_{d+1} z)(t, x) \right) \quad (5)$$

The main trick proposed (Li et al., 2020d) consists in using the convolution theorem to rewrite eq. (4) in terms of the  $(d + 1)$ -dimensional Fourier Transform  $\mathcal{F}_{d+1}$  and its inverse  $\mathcal{F}_{d+1}^{-1}$  (see definitions in Appendix A)

$$N_\theta^k(z)(t, x) = \sigma \left( A_\theta^k z(t, x) + b_\theta^k + \mathcal{F}_{d+1}^{-1} \left( \mathcal{F}_{d+1}(\mathcal{K}_\theta^k) \mathcal{F}_{d+1}(z) \right) (t, x) \right). \quad (6)$$

As argued in Li et al. (2020d), assuming that the kernel  $\mathcal{K}$  is periodic on  $[0, T] \times \mathcal{D}$ , instead of working with the Fourier Transform  $\mathcal{F}_{d+1}(\mathcal{K})$  we can consider its Fourier series expansion and truncate it at a maximal number of frequency modes  $\omega_1^{\text{max}}, \omega_2^{\text{max}}, \dots, \omega_{d+1}^{\text{max}} \in \mathbb{N}$ . This allows one to parameterize the evaluation  $\mathcal{F}_{d+1}(\mathcal{K}_\theta^k)(\omega)$  at any frequency mode  $\omega \in [0, T] \times \mathcal{D}$  directly as a complex  $(2\omega_1^{\text{max}} \times \dots \times 2\omega_{d+1}^{\text{max}} \times d_h \times d_h)$ -

tensor  $K_\theta^k$  and rewrite eq. (6) as follows

$$N_\theta^k(z)(t, x) = \sigma \left( A_\theta^k z(t, x) + b_\theta^k + \mathcal{F}_{d+1}^{-1} \left( K_\theta^k \mathcal{F}_{d+1}(z) \right) (t, x) \right), \quad (7)$$

where the multiplication  $K_\theta^k \mathcal{F}_{d+1}(z)$  is a matrix-vector multiplication<sup>3</sup>. Assuming uniform sampling of observations across space and time, we can approximate the Fourier Transform by the Fast Fourier Transform, as done in Li et al. (2020d, Section 4).

Despite the ability of FNOs to learn operators mapping either the initial condition  $u_0$  or a forcing term  $\xi$  to the solution  $u$  of a PDE, there is, however, no natural mechanism to adapt their architecture to learn solution operators mapping the pair  $(u_0, \xi)$  to the solution  $u$ , which is crucially needed to characterize SPDEs. Furthermore, as highlighted in the conclusion of Li et al. (2020d), for learning complex PDEs (such as SPDEs), FNOs require a large amount of training samples, which is hard to satisfy as data generation is generally a very expensive procedure. In addition, the number of learnable parameters in an FNO is usually very high, mainly because the weights are not shared among the different layers, making the model memory consuming and hard to train.

We note that an interesting line of work to tackle SPDE-learning is provided in the recent paper Chevyrev et al. (2021). The authors construct a set of features from the pair  $(u_0, \xi)$  following the definition of a model from the theory of regularity structures Hairer (2014). They then perform linear regression from this set of features to the solution of the SPDE at a specific point  $(t, x)$  in space-time. However, contrary to all other benchmarks considered in this paper, one would have to fit a different regression function for each space-time point. For this reason we do not include this recent line of work as one of our benchmarks.

In the Section 3 we provide a brief introduction to the theory of SPDEs which will help us defining our Neural SPDE model in Section 4.

### 3 Background on SPDEs

Let  $\mathcal{D} \subset \mathbb{R}^d$  be a bounded domain. Let  $\mathcal{H}_u = \{f : \mathcal{D} \rightarrow \mathbb{C}^{d_u}\}$  be a Hilbert space of functions on  $\mathcal{D}$  with values in  $\mathbb{C}^{d_u}$  and let  $\mathcal{H}_\xi = \{f : \mathcal{D} \rightarrow \mathbb{C}^{d_\xi}\}$  be a Hilbert space of functions on  $\mathcal{D}$  with values in  $\mathbb{C}^{d_\xi}$ .

We consider a large class of SPDEs of parabolic type

$$du = [-\mathcal{L}u + F(u)]dt + G(u)d\xi_t \quad (8)$$

where  $\xi_t$  is an infinite dimensional  $Q$ -Wiener process (Lord et al., 2014, Definition 10.6) or a cylindrical Wiener process (Hairer, 2009, Definition 3.54),  $F : \mathcal{H}_u \rightarrow \mathcal{H}_u$  and  $G : \mathcal{H}_u \rightarrow L(\mathcal{H}_\xi, \mathcal{H}_u)$  are two continuous functions, with  $L(\mathcal{H}_\xi, \mathcal{H}_u)$  denoting the space of bounded linear operators from  $\mathcal{H}_\xi$  to  $\mathcal{H}_u$ , and where  $-\mathcal{L}$  is a linear differential

<sup>3</sup>For any frequency mode  $\omega \in [0, T] \times \mathcal{D}$  one has  $\mathcal{F}_{d+1}(z)(\omega) \in \mathbb{C}^{d_h}$  and  $\mathcal{F}_{d+1}(K_\theta^k)(\omega) \in \mathbb{C}^{d_h \times d_h}$ .

operator generating a *semigroup*  $S_t$ . For a primer on semigroup theory see (Hairer, 2009, Section 4).

**Definition 1** A *strongly continuous semigroup*  $S$  on  $\mathcal{H}_u$  is a family of bounded linear operators  $S = \{S_t : \mathcal{H}_u \rightarrow \mathcal{H}_u\}_{t \geq 0}$  with the properties that

1.  $S_0 = Id$ , the identity operator on  $\mathcal{H}_u$ ,
2.  $S_t \circ S_s = S_{t+s}$ , for any  $s, t \geq 0$ ,
3. the function  $t \mapsto S_t u$  is continuous from  $[0, T]$  to  $\mathcal{H}_u$ , for any  $u \in \mathcal{H}_u$ .

A function  $u : [0, T] \rightarrow \mathcal{H}_u$  is a *mild solution* to the SPDE (8) if for any  $t \in [0, T]$

$$u_t = S_t u_0 + \int_0^t S_{t-s} F(u_s) ds + \int_0^t S_{t-s} G(u_s) d\xi_s, \quad (9)$$

where the integral is a stochastic integral (Hairer, 2009, Definition 3.57). An SPDE can be informally thought as a SDE with infinite dimensional state space  $\mathcal{H}_u$  and driven by an infinite dimensional "Brownian motion".

Assuming global Lipschitz regularity on the functions  $F$  and  $G$ , (Hairer, 2009, Theorem 6.4) guarantees the existence and uniqueness of a solution  $u : [0, T] \rightarrow \mathcal{H}_u$  to Equation (8). The proof relies on the Banach fixed point theorem (also known as the contraction mapping theorem) and works in almost exactly the same way as the usual proof of uniqueness of solution for ODEs with Lipschitz coefficients. The central argument in that proof, which is crucial for constructing our model in the next section, shows that under these conditions, the operator  $\Phi^\xi : C([0, T], \mathcal{H}_u) \rightarrow C([0, T], \mathcal{H}_u)$  depending on  $\xi$  and defined for any  $t \in [0, T]$  as

$$\Phi^\xi(u)_t := S_t u_0 + \int_0^t S_{t-s} F(u_s) ds + \int_0^t S_{t-s} G(u_s) d\xi_s \quad (10)$$

is a contraction, making the solution  $u$  of eq. (8) a fixed point for the operator  $\Phi^\xi$ , satisfying the identity  $u = \Phi^\xi(u)$ .

## 4 Neural SPDEs

Let  $m, n \in \mathbb{N}$ . Let  $D = \{x_1, \dots, x_m\} \subset \mathcal{D}$  be a  $m$ -points discretization of the spatial domain  $\mathcal{D}$ , and let  $\mathcal{T} = \{t_0, \dots, t_n\} \subset [0, T]$  be a  $(n+1)$ -points discretization of the time interval  $[0, T]$  with  $t_0 < \dots < t_n$ . Suppose the initial condition  $u_0 \in \mathcal{H}_u$  is observed on  $D$  and the forcing term  $\xi : [0, T] \rightarrow \mathcal{H}_\xi$  is observed on  $D$  at each time  $t_i \in \mathcal{T}$ .

Let  $\xi^\epsilon = \delta^\epsilon * \xi$  be the regularisation of  $\xi$  with a compactly supported smooth mollifier  $\delta^\epsilon$  scaled by  $\epsilon$  in space and  $\epsilon^2$  in time. From now on we take  $\mathcal{H}_u = L^2(\mathcal{D}, \mathbb{R}^{d_u})$  and

$\mathcal{H}_\xi = L^2(\mathcal{D}, \mathbb{R}^{d_\xi})$ . Replacing  $\xi$  by  $\xi^\epsilon$  in eq. (10) we get

$$\begin{aligned}\Phi^{\xi^\epsilon}(u)_t &= S_t u_0 + \int_0^t S_{t-s} F(u_s) ds + \int_0^t S_{t-s} G(u_s) \dot{\xi}_s^\epsilon ds \\ &= S_t u_0 + \int_0^t S_{t-s} H^{u, \xi^\epsilon}(s, \cdot) ds,\end{aligned}\tag{11}$$

where  $H^{u, \xi^\epsilon} : [0, T] \times \mathcal{D} \rightarrow \mathbb{C}^{d_u}$  is defined as

$$H^{u, \xi^\epsilon}(t, x) := (F(u_t) + G(u_t) \dot{\xi}_t^\epsilon)(x).\tag{12}$$

Renormalization is an important component of the theory of SPDEs which is very technical and goes beyond the scope of this article. The interested reader is referred to (Friz & Hairer, 2020, Section 15.5) for a detailed account of how this procedure works in the case of the KPZ equation. As far as the present article is concerned, the only thing to keep in mind is that for the solution  $u$  to exist in the limit when  $\epsilon \rightarrow 0$  one needs to introduce a (possibly infinite) normalization constant  $C_\epsilon \in \mathbb{R}^{d_u}$  – (Friz & Hairer, 2020, Theorem 15.2) – to the right-hand-side of eq. (11) to get our final version of  $\Phi$

$$\Phi^\epsilon(u)_t = C + S_t u_0 + \int_0^t S_{t-s} H^{u, \xi}(s, \cdot) ds\tag{13}$$

where we have dropped the dependency on  $\epsilon$  to ease notation. Hence, we can assume we are able to find a fine  $\epsilon$ -approximation to treat the SPDE (8) as an appropriately-renormalized PDE with forcing term  $\xi^\epsilon$ .

#### 4.1 Modelling the action of the semigroup $S$

For a large class of SPDEs, the action of the semigroup  $S$  can be written as a contraction against a kernel function  $\mathcal{K}_t : \mathcal{D} \times \mathcal{D} \rightarrow \mathbb{C}^{d_u \times d_u}$  such that for any  $h \in \mathcal{H}_u$

$$(S_t h)(x) = \int_{\mathcal{D}} \mathcal{K}_t(x, y) h(y) \mu_t(dy)\tag{14}$$

where  $\mu_t$  is a Borel probability measure on  $\mathcal{D}$ . Here, we take  $\mu_t$  to be the Lebesgue measure on  $\mathbb{R}^d$  but other choices can be made, for example to speed up computations or facilitate the learning process by incorporating prior information.

Several ways to parameterize the kernel functions  $\mathcal{K}$  have been introduced in the literature, for example using graph neural networks (Li et al., 2020b) or using the Fourier Transform (Li et al., 2020d). We follow the latter Fourier parameterization for the reasons mentioned in Section 2.5. For this, we assume that the kernel  $\mathcal{K} : [0, T] \times \mathcal{D} \rightarrow \mathbb{C}^{d_u \times d_u}$  is stationary in space and time so that  $\mathcal{K}_{t,s}(x, y) = \mathcal{K}_{t-s}(x - y)$ .

Hence, as observed in Section 2.5, equation (13) can be rewritten in terms of the



convolutions  $\star_d$  and  $\star_{d+1}$

$$\Phi^\xi(u)_t = C + \mathcal{K}_t \star_d u_0 + (\mathcal{K} \star_{d+1} H^{u,\xi})(t, \cdot) \quad (15)$$

By the convolution theorem, eq. (15) can be rewritten as

$$\Phi^\xi(u)_t = C + \mathcal{F}_d^{-1}(\mathcal{F}_d(\mathcal{K}_t)\mathcal{F}_d(u_0)) + \mathcal{F}_{d+1}^{-1}(\mathcal{F}_{d+1}(\mathcal{K})\mathcal{F}_{d+1}(H^{u,\xi}))(t, \cdot) \quad (16)$$

where both multiplications are matrix-vector multiplication.

Hence, as done for a single layer of a FNO, we parameterize the (evaluation of the) kernel  $\mathcal{K}$  directly in Fourier space as a complex tensor  $K_\theta$ . Doing so, eq. (16) becomes

$$\Phi_\theta^\xi(u)_t = C_\theta + \mathcal{F}_d^{-1}(\mathcal{F}_1^{-1}(K_\theta)_t \mathcal{F}_d(u_0)) + \mathcal{F}_{d+1}^{-1}(K_\theta \mathcal{F}_{d+1}(H_\theta^{u,\xi}))(t, \cdot) \quad (17)$$

where we used the fact that  $\mathcal{F}_d(\mathcal{K}_t) = \mathcal{F}_1^{-1}(\mathcal{F}_{d+1}(\mathcal{K}))(t)$ , for any  $t \in [0, T]$ , and used a subscript  $\theta$  to denote all elements of  $\Phi_\theta^\xi$  parameterized by learnable parameters.

It remains to discuss how to parameterize the function  $H_\theta^{u,\xi}$ .

## 4.2 Modelling the action of the vector fields $F$ and $G$

Recall that the function  $H^{u,\xi}$  is defined in eq. (12) in terms of the vector fields  $F : \mathcal{H}_u \rightarrow \mathcal{H}_u$  and  $G : \mathcal{H}_u \rightarrow L(\mathcal{H}_\xi, \mathcal{H}_u)$ , assume to satisfy some minimal Lipschitz conditions. For all the most common SPDEs arising from physics and finance, both  $F$  and  $G$  are local operators depending on  $u_t$  and its first spatial derivatives  $\partial u_t$ , in the sense that the evaluations  $F(u_t, \partial u_t)(x)$  and  $G(u_t, \partial u_t)(x)$  at a point  $x \in \mathcal{D}$  only depend on the evaluations  $u_t(x)$  and  $\partial u_t(x)$  at  $x$ , and not on their evaluations at some other point  $y \in \mathcal{D}$  in the neighbourhood of  $x$ . Typical examples of  $F$  and  $G$  are polynomials in  $u_t(x)$  and  $\partial u_t(x)$ .

Thanks to the properties of the Fourier Transform  $\mathcal{F}_d(u_t)$ , it is easy to augment  $u_t$  with its first derivatives to  $[u_t, \partial u_t]$

$$\partial u_t = \mathcal{F}_d^{-1}(\alpha \omega \mathcal{F}_d(u_t)) \quad (18)$$

where  $\alpha \in \mathbb{C}$  is a complex constant.

Hence, we can model the action of  $F$  and  $G$  as neural networks  $F_\theta : \mathbb{C}^{d_u(d+1)} \rightarrow \mathbb{C}^{d_u}$  and  $G : \mathbb{C}^{d_u(d+1)} \rightarrow \mathbb{C}^{d_u \times d_\xi}$  acting on  $[u_t, \partial u_t](x) \in \mathbb{C}^{d_u(d+1)}$ , i.e.

$$\begin{aligned} F(u_t)(x) &\approx F_\theta([u_t, \partial u_t](x)) \\ (G(u_t)\dot{\xi}_t)(x) &\approx G_\theta([u_t, \partial u_t](x))\dot{\xi}_t(x) \end{aligned}$$

In summary

$$\begin{aligned} H_\theta^{u,\xi}(t, x) &= F_\theta \left( [u_t, \mathcal{F}_d^{-1}(\alpha\omega\mathcal{F}_d(u_t))](x) \right) \\ &\quad + G_\theta \left( [u_t, \mathcal{F}_d^{-1}(\alpha\omega\mathcal{F}_d(u_t))](x) \right) \dot{\xi}_t(x) \end{aligned} \quad (19)$$

### 4.3 A neural fixed point problem

Our final Neural SPDE model consists of three components: a lift  $L_\theta : \mathbb{R}^{d_u+1} \rightarrow \mathbb{R}^{d_h}$  to a hidden state  $\mathbb{R}^{d_h}$ , an operator  $\Phi_\theta^\xi$  given by combining expressions (17) and (19), and a projection  $\Pi_\theta : \mathbb{R}^{d_h} \rightarrow \mathbb{R}^{d_u}$  back to the original space  $\mathbb{R}^{d_u}$ .

The operator  $\Phi_\theta^\xi$  is used to solve a fixed point problem  $z = \Phi_\theta^\xi(z)$  whose solution  $z$  is a mild solution of an SPDE. Algorithmically, we proceed by Picard’s iteration

$$z_t^i(x) = L_\theta(u_t^{\text{in}}(x)), \quad z_t^{i+1}(x) = \Phi_\theta^\xi(z_t^i)_t(x), \quad u_t^{\text{out}}(x) = \Pi_\theta(z_t^M(x)) \quad (20)$$

for any  $t \in [0, T]$ ,  $x \in \mathcal{D}$  and  $i = 0, \dots, M-1$ .

The crucial difference between the Neural SPDE model of eq. (20) and a Neural SDE model of Section 2.3 is that in the former the solution  $u_t$  and the noise  $\xi_t$  take their values in functional spaces  $\mathcal{H}_u, \mathcal{H}_\xi$  respectively, while in the latter  $u_t$  and  $\xi_t$  are vector-valued. We note that a Neural SDE could be used in the context of SPDE-learning by considering the evaluations of  $u_t$  and  $\xi_t$  on a discretized grid  $D$  as state space of the SDE dynamics. However this would result in a procedure that is not resolution-invariant. Furthermore, as shown in the experimental section below, Neural SDEs in such high dimensional state spaces are very hard to train and yield very poor performance compared to all other considered models.

The crucial difference between the Neural SPDE model of eq. (20) and the FNO model of eq. (3) is between the Neural SPDE operator  $\Phi_\theta$  and the FNO operator  $N_\theta^M \circ \dots \circ N_\theta^1$ . Firstly, by construction,  $\Phi_\theta$  operates on the pair  $(z, \xi)$ , whilst the FNO operator is built to act on  $z$  alone (or possibly on  $\xi$  alone) and so it can’t be used to handle solution operators for SPDEs. Secondly, each FNO layer  $N_\theta^i$  consists of a non-linear image of an affine transformation involving a local operation and a global operation, which doesn’t represent any physical mechanism (resulting in poor performance when learning complex PDE dynamics, as shown in the next section), whilst  $\Phi_\theta$  encodes real physical dynamics as it is precisely the (mild) solution operator of an SPDE. Thirdly, the number of learnable parameters in an FNO is approximately  $M$  times larger than in a Neural SPDE, which is much less expensive as weights are naturally shared across iterations.

## 5 Experiments

In this section we demonstrate how our Neural SPDE model can be used in three different supervised learning settings:

1. learn the operator  $u^{\text{in}} \mapsto u^{\text{out}}$  (assuming the underlying noise  $\xi$  is not observed),

2. learn the operator  $\xi \mapsto u^{\text{out}}$  (assuming the underlying noise  $\xi$  is observed but the prior data  $u^{\text{in}}$  is fixed across samples),
3. learn the operator  $(u^{\text{in}}, \xi) \mapsto u^{\text{out}}$  (assuming the underlying noise  $\xi$  is observed and that the prior data  $u^{\text{in}}$  changes across samples).

Later on in the section we showcase how the Neural SPDE model can also be used as a generator in a conditional generative modelling setting to produce randomly sampled solutions  $\{u_i^{\text{out}}\}_{i=1}^n$  matching the distributional behaviour of some observed solutions  $\{u_i^{\text{true}}\}_{i=1}^m \sim \mathbb{P}$  of an underlying unknown SPDE, conditioned  $u_i^{\text{in}}$ .

## 5.1 Supervised learning

For every supervised learning problem we use the un-normalized pathwise L2 loss. We use the Adam optimizer to train for 500 epochs with an initial learning rate of 0.001 that is halved every 100 epochs. For all models the readin and readout maps as well as the vector fields are modelled as feedforward neural networks. The feedforward neural networks for the readin and the readout maps have one and two layers respectively. In the  $\Phi_1^4$  example, for all models we use  $d_h = 16$  hidden units. For FNO and Neural SPDE we use the 32 maximal frequency modes both in space and time. For FNO we stack four integral operator layers as in Li et al. (2020d). For Neural SPDE we use 4 Picard’s iterations. For the Navier-Stokes example, we use the maximal 16 frequencies in space, the maximal 10 frequencies in time and  $d_h = 8$ .

### 5.1.1 Dynamic $\Phi_1^4$ model

We start with the dynamic  $\Phi_1^4$  model in 1D which is denoted by  $\Phi_1^4$  and is given by,

$$\begin{aligned} \partial_t u(t, x) - \Delta u(t, x) &= 3u(t, x) - u(t, x)^3 + u(t, x)\dot{\xi}(t, x), & (t, x) &\in [0, T] \times \mathbb{T} \\ u(0, x) &= u_0(x), & x &\in \mathbb{T} \end{aligned} \quad (21)$$

where  $\mathbb{T}$  denotes the 1-dimensional torus, i.e.  $[0, 1]$  with endpoints identified ( $\mathbb{T} = \mathbb{R}/\mathbb{Z}$ ). Here  $\xi$  is a space-time white noise, and we use the approximation given in Lord et al. (2014, Example 10.31) to sample realizations from this process. We then solve the SPDE for each sample path using a finite difference method with 128 evenly distanced points in space and a time step  $\Delta t = 10^{-3}$ . We solve the SPDE until  $T = 0.05$  resulting in 50 time points. In the case where the initial data  $u^{\text{in}}(t, x) = u_0(x)$  is fixed across samples, we take  $u_0(x) = x(1 - x)$ . In the case where it varies across samples, we add a random term  $u_0(x) = x(1 - x) + \eta(x)$  where

$$\eta(x) = 0.1 \sum_{k=-10}^{k=10} \frac{a_k}{1 + |k|^2} \sin(\lambda^{-1} k \pi (x - 0.5)), \quad \text{with } a_k \sim \mathcal{N}(0, 1)$$

similar to Chevyrev et al. (2021, Equation (3.6)) with  $\lambda = 2$ .

We report the results in Table 1. The Neural SPDE model (NSPDE) obtains the lowest relative error for all tasks, and obtains nearly one order of magnitude lower relative error

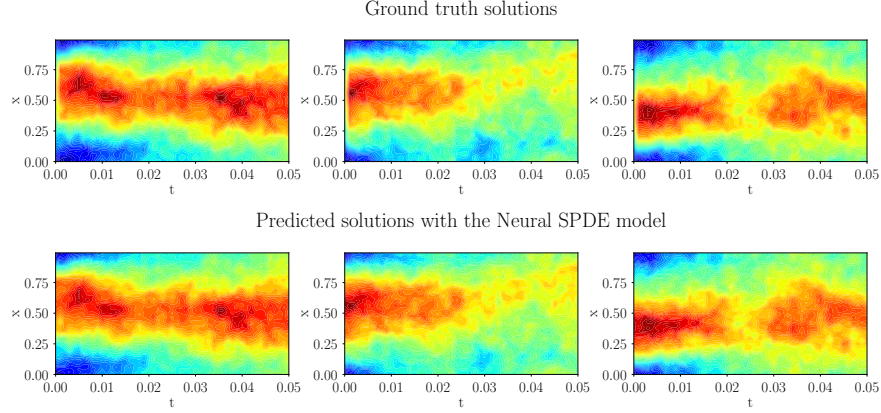


Figure 1: Ground truth and predictions on three test instances for the  $\Phi_1^4$  example.

compared to Neural CDE models (NCDE). We note that the Neural SPDE is the only model that can be applied to the three considered supervised learning settings.

### 5.1.2 Stochastic Navier-Stokes in 2D

We consider the vorticity equation for an incompressible two-dimensional flow,

$$\begin{aligned} \partial_t w(t, x) - \nu \Delta w(t, x) &= -u(t, x) \cdot \nabla w(t, x) + f(x) + \sigma \dot{\xi}(t, x), \quad (t, x) \in [0, T] \times \mathbb{T}^2 \\ w(0, x) &= w_0(x), \quad x \in \mathbb{T}^2 \end{aligned} \quad (22)$$

where  $\mathbb{T}^2$  denotes the 2-dimensional torus, i.e.  $[0, 1]^2$  with opposite sides identified ( $\mathbb{T}^2 = \mathbb{R}^2 / \mathbb{Z}^2$ ). The system is subject to both deterministic and random forces. The deterministic force  $f$  is a function of space only and is defined as in Li et al. (2020d). The additive stochastic forcing term  $\xi$  depends on both time and space and is a Q-Wiener process which is colored in space and rescaled by  $\sigma = 0.05$ . We take the Q-Wiener process defined in Lord et al. (2014, Example 10.12) with  $\alpha = 0.005$ . The initial condition  $w_0$  is generated according to  $w_0 \sim \mathcal{N}(0, 3^{3/2}(-\Delta + 49I)^{-3})$  with periodic boundary conditions. The viscosity parameter is set to  $\nu = 10^{-4}$ .

We use Lord et al. (2014, Algorithm 10.6) to approximate sample paths from the Q-Wiener process. For each sample path we solve (22) with a pseudo-spectral solver (adapted from Li et al. (2020d)) where time is advanced with a Crank–Nicolson update. We solve the SPDE on a  $64 \times 64$  mesh in space and use a time-step of  $10^{-3}$  for the Crank–Nicolson scheme. We generate 10 long trajectories of 15 000 steps each from  $t = 0$  to  $t = 15$ . We partition each of these 10 trajectories into consecutive sub-trajectories of 500 time-steps using a rolling window. This procedure yields a total of 2 000 input-output pairs. We chose to split the data into shorter sequences of 500 time steps so that one batch training could fit in memory on a Tesla P100 NVIDIA GPU. However, the model shows good performance (see Figure 2) even when evaluated on a 5 000 time

Table 1: **Dynamic  $\Phi_1^4$  model.** We report the relative L2 error on the test set. The symbol  $\times$  indicates that the model is not applicable. In the first task ( $u_0 \mapsto u$ ) only partial information ( $u_0$ ) is provided as input; the underlying noise  $\xi$  is used to generate the dynamics, it varies across samples, but is not provided as an input to the models. This explains why the performance of the applicable models (FNO and NSPDE) is poorer than for all other settings. In the second setting, ( $\xi \mapsto u$ ) the initial condition  $u_0$  is kept fixed. In the third setting, the initial condition  $u_0$  and the noise  $\xi$  change and are both provided as input to the model. In these last two settings, even with a limited amount of training samples ( $N = 1000$ ), the NSPDE model is able to achieve  $\sim 1\%$  error rate, and even marginally improves to  $< 1\%$  error when  $N = 10000$ . This indicates that our model is able to capture complex dynamics even in a small data regime.

Model	$N = 1000$			$N = 10000$		
	$u_0 \mapsto u$	$\xi \mapsto u$	$(u_0, \xi) \mapsto u$	$u_0 \mapsto u$	$\xi \mapsto u$	$(u_0, \xi) \mapsto u$
NCDE-linear	x	0.112	0.127	x	0.056	0.072
NCDE-spline	x	0.110	0.128	x	0.056	0.070
NRDE (depth 2)	x	x	x	x	x	x
FNO	0.128	0.032	x	0.126	0.027	x
NSPDE (Ours)	0.128	<b>0.009</b>	<b>0.012</b>	0.126	<b>0.006</b>	<b>0.006</b>

step period. To showcase zero-shot super-resolution, we train the Neural SPDE model on a downsampled version of the data with  $16 \times 16$  spatial resolution. After training on this coarser resolution we evaluate the model on the original resolution as shown in Figure 2. We can see that even if trained on a lower resolution the model is capable of learning the stochastic Navier-Stokes dynamics on a finer resolution.

## 5.2 Generative model

In this last section we discuss how one can use the Neural SPDE model as generator to model random solutions of an SPDE. A generative adversarial network (GAN) learns to generate new data with the same "statistics" as the data observed in the training set. A GAN has two main components: 1) a generator trying to minimize a distance between the generated and true datasets and 2) a discriminator trying to maximize this distance, hence acting adversarially.

**Generator** Here we use a Neural SPDE as generator to map sample paths from space-time white noise  $\xi$  to sample solutions  $u^{\text{out}}$  conditioned on prior data  $u^{\text{in}}$ .

**Discriminator** There are several variants of GAN consisting of different choices of discriminator: Wasserstein-GAN Arjovsky et al. (2017) uses the Wasserstein distance, MMD-GAN Li et al. (2017) uses the maximum mean discrepancy (MMD). The signature kernel  $k_{\text{sig}}$  Salvi et al. (2021a) provides a natural kernel for high dimensional paths and

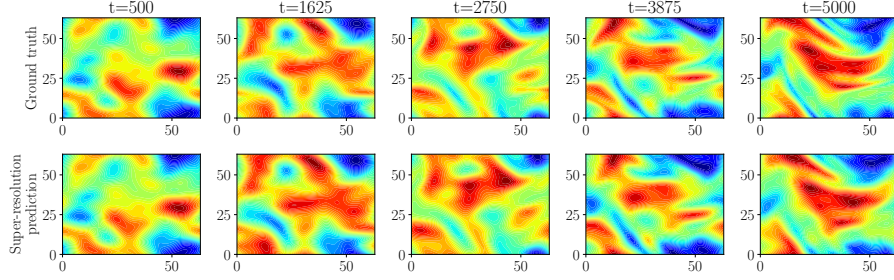


Figure 2: **Top panel:** Solution of the vorticity equation for one realisation of the stochastic forcing between the 500<sup>th</sup> and the 5 000<sup>th</sup> time steps. **Bottom panel:** Predictions with the Neural SPDE model given the initial condition at the 500<sup>th</sup> time step and the forcing between the 500<sup>th</sup> and the 5 000<sup>th</sup> time steps. The model has been trained on lower resolution data, with a  $16 \times 16$  mesh and is evaluated on a  $64 \times 64$  mesh.

the resulting signature-MMD

$$D_{k_{\text{sig}}}(\mathbb{P}, \mathbb{Q}) = \mathbb{E}_{\mathbb{P}}[k_{\text{sig}}(x, x')] - 2\mathbb{E}_{\mathbb{P}, \mathbb{Q}}[k_{\text{sig}}(x, x')] + \mathbb{E}_{\mathbb{Q}}[k_{\text{sig}}(y, y')] \quad (23)$$

is a natural metric for comparing distributions of path space Salvi et al. (2021b). We use the latter as discriminator to train our generative model by considering  $u^{\text{in}}, u^{\text{out}}, u^{\text{true}}$  as paths<sup>4</sup> evolving on  $D \times \mathbb{R}^{d_u}$ .

For simplicity let's assume we do not condition on prior data. So we assume we are given  $n$  solution samples  $\{(u_i^{\text{true}})\}_{i=1}^n \sim \mathbb{P}_{\text{true}}$ . Then we simulate  $m$  space-time white noise sample  $\{\xi_i\}_{i=1}^m \sim \mathbb{P}_{\text{noise}}$  and feed them to a first Neural SPDE to obtain  $\mathbb{P}_{\text{out}} = \text{NSPDE}_{\theta}^1(\mathbb{P}_{\text{noise}})$ . We then use a second Neural SPDE ( $\text{NSPDE}_{\phi}^2$ ) to help the discriminator and learn by playing a two-player game where  $\text{NSPDE}_{\phi}^2$  tries to distinguish between  $\mathbb{P}_{\text{out}}$  and  $\mathbb{P}_{\text{true}}$ , whilst  $\text{NSPDE}_{\theta}^1$  tries to confuse  $\text{NSPDE}_{\phi}^2$ . In other words we use the following objective loss

$$\min_{\theta} \max_{\phi} D_{k_{\text{sig}} \circ \text{SPDE}_{\theta}^1}(\mathbb{P}_{\text{out}}, \mathbb{P}_{\text{true}}) \quad (24)$$

### 5.2.1 KPZ equations

We consider the Kardar-Parisi-Zhang (KPZ) equations,

$$\begin{aligned} \partial_t u(x, t) &= \nu \nabla^2 u(x, t) + \frac{\lambda}{2} (\nabla u(x, t))^2 + \sigma \dot{\xi}(x, t), & t \in [0, T], x \in (0, 1) \\ u(x, 0) &= u_0(x), & x \in (0, 1). \end{aligned}$$

<sup>4</sup>Note that this procedure is resolution-invariant. Also the complexity of computing the sig-MMD is linear in the dimensionality of the input sample paths.

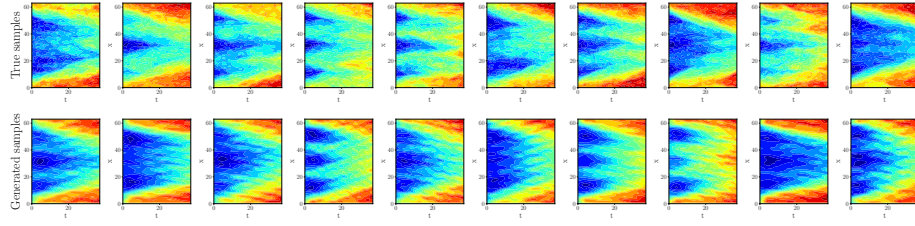


Figure 3: **Top panel:** Sample solutions of the KPZ equation obtained with the py-pde numerical solver. **Bottom panel:** Samples produced by the Neural SPDE-GAN.

We use the py-pde Python package (Zwicker, 2020) to generate solutions of the KPZ equations with  $(\nu, \lambda, \sigma) = (0.5, 3, 0.2)$ . We use the 32 maximal frequencies in both space and time,  $d_h = 32$  hidden channels and 2 Picard’s iterations. The batch size is 128.

## References

- Arjovsky, M., Chintala, S., and Bottou, L. Wasserstein generative adversarial networks. In *International conference on machine learning*, pp. 214–223. PMLR, 2017.
- Chen, R. T., Rubanova, Y., Bettencourt, J., and Duvenaud, D. Neural ordinary differential equations. In *Proceedings of the 32nd International Conference on Neural Information Processing Systems*, pp. 6572–6583, 2018.
- Chevyrev, I., Gerasimovics, A., and Weber, H. Feature engineering with regularity structures. *arXiv preprint arXiv:2108.05879*, 2021.
- Ciccone, M., Gallieri, M., Masci, J., Osendorfer, C., and Gomez, F. Nais-net: Stable deep networks from non-autonomous differential equations. *arXiv preprint arXiv:1804.07209*, 2018.
- Friz, P. K. and Hairer, M. *A course on rough paths*. Springer, 2020.
- Hairer, M. An introduction to stochastic pdes. *arXiv preprint arXiv:0907.4178*, 2009.
- Hairer, M. Solving the kpz equation. *Annals of mathematics*, pp. 559–664, 2013.
- Hairer, M. A theory of regularity structures. *Inventiones mathematicae*, 198(2):269–504, 2014.
- Holden, H., Øksendal, B., Ubøe, J., and Zhang, T. Stochastic partial differential equations. In *Stochastic partial differential equations*, pp. 141–191. Springer, 1996.
- Kidger, P., Morrill, J., Foster, J., and Lyons, T. Neural controlled differential equations for irregular time series. *arXiv preprint arXiv:2005.08926*, 2020.
- Kidger, P., Foster, J., Li, X., and Lyons, T. Efficient and accurate gradients for neural sdes. *arXiv preprint arXiv:2105.13493*, 2021a.

- Kidger, P., Foster, J., Li, X., Oberhauser, H., and Lyons, T. Neural sdes as infinite-dimensional gans. *arXiv preprint arXiv:2102.03657*, 2021b.
- Kleinert, H. and Schulte-Frohlinde, V. *Critical properties of  $\phi^4$ -theories*. World Scientific, 2001.
- Kovachki, N., Li, Z., Liu, B., Azizzadenesheli, K., Bhattacharya, K., Stuart, A., and Anandkumar, A. Neural operator: Learning maps between function spaces. *arXiv preprint arXiv:2108.08481*, 2021.
- Li, C.-L., Chang, W.-C., Cheng, Y., Yang, Y., and Póczos, B. Mmd gan: Towards deeper understanding of moment matching network. *arXiv preprint arXiv:1705.08584*, 2017.
- Li, X., Wong, T.-K. L., Chen, R. T., and Duvenaud, D. Scalable gradients for stochastic differential equations. In *International Conference on Artificial Intelligence and Statistics*, pp. 3870–3882. PMLR, 2020a.
- Li, Z., Kovachki, N., Azizzadenesheli, K., Liu, B., Bhattacharya, K., Stuart, A., and Anandkumar, A. Neural operator: Graph kernel network for partial differential equations. *arXiv preprint arXiv:2003.03485*, 2020b.
- Li, Z., Kovachki, N., Azizzadenesheli, K., Liu, B., Stuart, A., Bhattacharya, K., and Anandkumar, A. Multipole graph neural operator for parametric partial differential equations. *Advances in Neural Information Processing Systems*, 33, 2020c.
- Li, Z., Kovachki, N. B., Azizzadenesheli, K., Bhattacharya, K., Stuart, A., Anandkumar, A., et al. Fourier neural operator for parametric partial differential equations. In *International Conference on Learning Representations*, 2020d.
- Lord, G. J., Powell, C. E., and Shardlow, T. *An introduction to computational stochastic PDEs*, volume 50. Cambridge University Press, 2014.
- Lyons, T. Rough paths, signatures and the modelling of functions on streams. *arXiv preprint arXiv:1405.4537*, 2014.
- Lyons, T. J. Differential equations driven by rough signals. *Revista Matemática Iberoamericana*, 14(2):215–310, 1998.
- Lyons, T. J., Caruana, M., and Lévy, T. *Differential equations driven by rough paths*. Springer, 2007.
- Mikulevicius, R. and Rozovskii, B. L. Stochastic navier–stokes equations for turbulent flows. *SIAM Journal on Mathematical Analysis*, 35(5):1250–1310, 2004.
- Morrill, J., Salvi, C., Kidger, P., and Foster, J. Neural rough differential equations for long time series. In *International Conference on Machine Learning*, pp. 7829–7838. PMLR, 2021.
- Pontryagin, L. S. *Mathematical theory of optimal processes*. CRC press, 1987.
- Salvi, C., Cass, T., Foster, J., Lyons, T., and Yang, W. The signature kernel is the solution of a goursat pde. *SIAM Journal on Mathematics of Data Science*, 3(3): 873–899, 2021a.



- Salvi, C., Lemerrier, M., Liu, C., Hovarth, B., Damoulas, T., and Lyons, T. Higher order kernel mean embeddings to capture filtrations of stochastic processes. *arXiv preprint arXiv:2109.03582*, 2021b.
- Zwicker, D. py-pde: A python package for solving partial differential equations. *Journal of Open Source Software*, 5(48):2158, 2020.

## A Fourier Transform

Let  $V$  be a vector space over the complex numbers; in what follows  $V$  will be either  $\mathbb{C}^{d_u}$  or  $\mathbb{C}^{d_u \times d_u}$ . Let  $r \in \mathbb{N}$  and let  $\mathcal{C} \subset \mathbb{R}^r$  be a compact subset of  $\mathbb{R}^r$ . In the paper we used either  $r = d$  and  $\mathcal{C} = \mathcal{D}$  or  $r = d + 1$  and  $\mathcal{C} = [0, T] \times \mathcal{D}$ .

The  $r$ -dimensional Fourier Transform  $\mathcal{F}_r : L^2(\mathcal{C}, V) \rightarrow L^2(\mathcal{C}, V)$  and its inverse  $\mathcal{F}_r^{-1} : L^2(\mathcal{C}, V) \rightarrow L^2(\mathcal{C}, V)$  are defined as follows

$$\mathcal{F}_r(f)(y) = \int_{\mathcal{C}} e^{-2\pi i \langle x, y \rangle} f(x) dx, \quad (25)$$

$$\mathcal{F}_r^{-1}(g)(x) = \int_{\mathcal{C}} e^{2\pi i \langle x, y \rangle} g(y) dy \quad (26)$$

for any  $f, g \in L^2(\mathcal{C}, V)$ , where  $i = \sqrt{-1}$  is the imaginary unit and  $\langle \cdot, \cdot \rangle$  denotes the Euclidean inner product on  $\mathbb{R}^r$ .

## B Deterministic Navier Stokes

Here we demonstrate that our Neural SPDE model can also be used in the setting of PDEs without any stochastic term, reducing to a Neural PDE model. We do so by studying the example from Li et al. (2020d) on deterministic Navier-Stokes. More precisely, we consider the 2D Navier-Stokes equation for a viscous, incompressible fluid in vorticity form on the 2-dimensional torus:

$$\partial_t w(t, x) - \nu \Delta w(t, x) = f(x) - u(t, x) \cdot \nabla w(t, x), \quad t \in [0, T], x \in \mathbb{T}^2 \quad (27)$$

$$\nabla \cdot u(t, x) = 0, \quad t \in [0, T], x \in \mathbb{T}^2 \quad (28)$$

$$w(x, 0) = w_0(x), \quad x \in \mathbb{T}^2 \quad (29)$$

where  $u : [0, T] \times \mathbb{T}^2 \rightarrow \mathbb{R}^2$  is the velocity field,  $w = \nabla \times u$  is the vorticity with  $w_0 : \mathbb{T}^2 \rightarrow \mathbb{R}$  being the initial vorticity. Here  $f$  is a deterministic forcing term which we take as in Li et al. (2020d). Compared to the Navier-Stokes equations we consider in Section 5, there is no stochastic forcing term. We follow the experimental setup from Li et al. (2020d) and use the dataset where  $\nu = 10^{-5}$ ,  $N = 1000$  and  $T = 20$ . We achieve similar performances as FNO with a L2 error of 0.17.

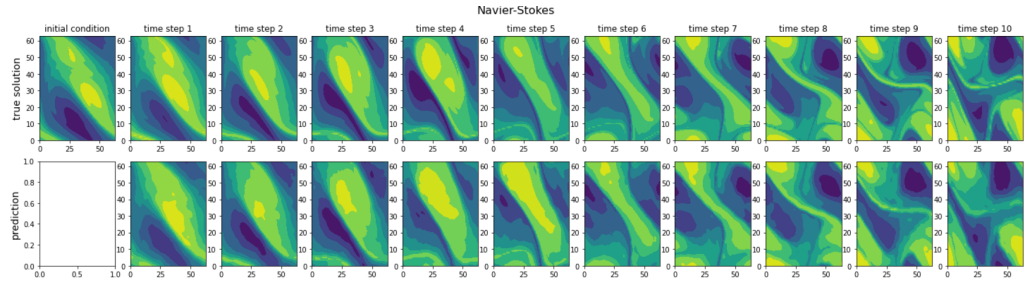


Figure 4: **Top panel:** Initial vorticity and ground truth vorticity at later time steps on a  $64 \times 64$  mesh. **Bottom panel:** Predictions of the Neural SPDE model.